Differential cross sections for elastic electron scattering in xenon in the energy range from 5 eV to 10 eV

Ireneusz Linert,[1] Brygida Mielewska,[1] George C. King,[2] and Mariusz Zubek[1]
[1]*Department of Physics of Electronic Phenomena, Gdańsk University of Technology, 80-952 Gdańsk, Poland*
[2]*School of Physics and Astronomy, Schuster Laboratory, Manchester University, Manchester M13 9PL, United Kingdom*
(Received 10 July 2007; published 27 September 2007)

Differential cross sections for elastic electron scattering in xenon have been measured at the energies of 5, 7.9, and 10 eV over the scattering angle range from 30° to 180°. For the measurements in the backward-angle scattering range the magnetic angle-changing technique has been employed. The differential cross sections obtained have been integrated to yield the elastic integral and momentum transfer cross sections. A detailed comparison of the present differential and integral cross sections is made with the existing experimental data and the results of various theoretical calculations. This comparison indicates that the theoretical results achieve a better overall agreement with the experimental cross sections in the backward scattering region than for the case of argon.

DOI: 10.1103/PhysRevA.76.032715 PACS number(s): 34.80.Bm

I. INTRODUCTION

Studies of electron scattering processes from noble gas atoms are important from the point of developing adequate theoretical models of the interactions of electrons with closed-shell atoms. This is particularly the case at low electron energies, <10 eV. The electron-atom interactions are expressed in terms of absolute differential, integral, and momentum transfer cross sections, which also contain valuable information on the dynamics of the scattering process. Heavy atoms exhibit strong variations in their elastic cross sections with respect to angular (see, for example, [1] for the case of mercury) and low-energy dependencies and provide sensitive tests for the theoretical description of the interactions. In the case of xenon the differential cross sections display distinct minima at about 120° and the integral cross sections show a Ramsauer-Townsend minimum at 0.8 eV and a broad maximum at about 6.5 eV [2]. Also, the existing theoretical calculations predict that the differential cross sections will increase to a maximum value at a scattering angle of 180°. It is expected that in the backward scattering region, and at low incident electron energies (<10 eV) correlation-polarization interactions will dominate the scattering. Thus experiments which provide differential cross sections up to 180° give important physical insights into these interactions.

As a continuation of our studies of electron elastic scattering in the noble gases [3,4], in this work we present measurements of the differential cross sections for elastic scattering in xenon performed over a wide angular range from 30° to 180° at incident electron energies of 5, 7.9, and 10 eV. These are the first measurements of the elastic cross section obtained up to 180° for energies below 10 eV. In the range of backward scattering the measurements have been performed with the application of the magnetic angle-changing technique [5]. Absolute values of the cross sections have been evaluated using the relative flow technique. Comparison of our previous measurements carried out in the region of backward scattering for neon [4] and argon [3] with theoretical calculations of the differential cross sections have revealed that in the lighter atom neon there is an overall good agreement between experimental and theoretical results. However, the theoretical calculations in argon tend to overestimate the cross sections. This overestimation of the cross sections causes the integrated elastic cross sections to lie above the measured total cross sections. The present work allows experimental cross sections for the heavier atom xenon to be compared with the theoretical calculations and in particular, for the backward scattering region.

Historically, the first measurements of elastic differential cross sections for electron scattering in xenon in the low-energy range (≤ 10 eV) were performed in the early 1930s in the pioneering work of Ramsauer and Kollath [6] in an exceptionally wide angular range from 15° to 167.5°. More recently Mehr [7], Heindorff *et al.* [8], and Klewer *et al.* [9] presented relative differential cross sections in the scattering angle range up to typically 140°, while Register *et al.* [10], Nishimura *et al.* [11], Weyhreter *et al.* [12], and Gibson *et al.* [13] presented absolute cross sections over a similar range. Very recently Cho *et al.* [14] used the magnetic angle-changing technique to measure the cross sections from 20° to 180° at energies of 10 eV and above.

The theoretical calculations of elastic electron scattering in xenon have been carried out using various approximations to include correlation-polarization, exchange, and relativistic interactions, since the early relativistic work of Walker [15]. More recently the polarized-orbital method has been used by McEachran and Stauffer [16] within their adiabatic exchange approximation, which included dipole polarization and treated exchange exactly. These authors have also, in their latter calculations, which took the relativistic approach but with nonrelativistic polarization potential, obtained elastic scattering phase shifts to determine the spin polarization parameters [17] and integral elastic and momentum transfer cross sections [18]. A further developed version of the polarized-orbital method of McEachran and Stauffer has been applied by these authors to xenon [13]. These are fully relativistic calculations, which include both static and dynamic polarization effects. This approach has been used most recently by Cho *et al.* [14] in their calculations, which also took into account the absorption effects via a complex opti-

cal potential, for elastic scattering in xenon in the intermediate energy range (10–100 eV). A different variation of the polarized-orbital approach has been used by Sin Fai Lam [19] in semirelativistic calculations with direct relativistic effects described by the second-order Dirac potential. Gianturco and Rodriguez-Ruiz [20] in their nonrelativistic theoretical approach used a model exchange potential based on a free-electron-gas system. They described the short-range correlation-polarization interaction using density-functional theory while the long-range correlation-polarization interaction was treated adiabatically (up to the octupole polarization term). Charge density functionals have been applied to introduce an exchange-correlation potential by Haberland *et al.* [21] in Kohn-Sham–type relativistic one-particle calculations. Johnson and Guet [22] employed many-body perturbation theory to account for the electron correlation in their calculations. Correlation-polarization interaction has also been described in a number of theoretical works by applying model potentials. Yuan and Zhang applied a nonrelativistic approach [23] and also a quasirelativistic approach [24] treating exchange interaction exactly and accounting for correlation, distortion, and polarization effects by a parameter-free correlation-polarization potential of Padial and Norcross [25]. This is a modification of that used by O'Connell and Lane [26] in their calculations of the integral cross section in xenon. Sienkiewicz and Baylis [27] in their Dirac-Fock method used a model potential which incorporates the dipole polarization and exchange-polarization terms and treated exchange exactly. Finally, Berg [28] made use of X_α potential representing exchange and correlation interactions.

II. EXPERIMENT

The present measurements have been carried out with an electrostatic electron spectrometer used in conjunction with a magnetic angle changer, which produces a localized, static magnetic field at the interaction region. The crucial feature of this device is that the incident and scattered electrons are deflected in the magnetic field by a certain angle and this allows electrons scattered in the backward hemisphere to be detected [29].

The apparatus has been described in detail previously [30]. The electron spectrometer consists of an electron monochromator that is fixed in position and a rotatable electron energy analyzer. This analyzer covers the angular range from −10° to 120° with respect to the direction of the incident electron beam. The monochromator employs a hemispherical selector of mean radius 50 mm. The electron beam from the selector is focused onto the target gas beam by two triple-aperture lenses. Electrons scattered from the target gas are decelerated and focused by a three-element cylindrical lens onto the entrance of a hemispherical selector of mean radius 20 mm. Transmitted electrons are detected by channel electron multiplier. The target gas beam is formed by a single capillary of internal diameter of 0.3 mm and length 10 mm. The energy resolution of the present elastic scattering measurements was 80 meV at an incident beam current of typically 5 nA. The incident electron energy was calibrated at regular intervals on the ^2S resonance in helium and is accurate to ±30 meV.

The magnetic angle changer used in these measurements has been described in detail by Linert *et al.* [5]. It consists of two pairs of coaxial solenoids of conical geometry to produce the localized and shaped magnetic field at the interaction region. The magnetic field produced by this solenoid system decreases very rapidly with radial distance from the scattering region and reaches 0.1% of its value at the scattering region at a distance of 40 mm. In such type of a magnetic field, the electrons that are incident on the target region and the scattered electrons are deflected by a certain angle. The total deflection angle of the electrons of 70° combined with the angular range of rotation of the analyzer (−10°–120°) allows the detection of scattered electrons over the full angular range, including 180°. The angular scale of the present measurements was calibrated with respect to the two minima in the elastic differential cross sections of argon that occur at 117.5° at 10 eV and at 72.5° at 15 eV. The total uncertainty in the angular scale and the angular resolution are estimated to be ±2° and 4°, respectively.

In order to determine the differential cross sections for elastic scattering in xenon the intensities of scattered electrons with respect to those in helium, which was used as the reference gas, were measured at each scattering angle, at intervals of 10° over the angular range 30°–180°. Simultaneously, the corresponding flow rates of both gases were determined. These relative intensities and the calculated cross sections of Nesbet [31] were then used to obtain absolute cross sections in xenon according to the relative flow technique [32,33]. The gas flow rates were determined from the measurements of the rate of pressure increase in a volume of a section of gas line using a Baratron pressure gauge. The driving pressures behind the beam-forming capillary for xenon were maintained below 11 Pa. In the relative flow method the requirement of equal mean-free-path lengths in the capillary for the gas under investigation and the reference gas must be fulfilled. For the case of xenon, the required ratio of its driving pressure to helium was equal to 0.2. During the measurements both the xenon and helium gases were always present in the vacuum chamber to ensure the operational stability of the electron spectrometer. Here, one gas was admitted to the scattering region through the capillary and the other to the vacuum chamber through a side valve. The contributions from the background gas in the interaction region were determined for each measurement by admitting both gases directly into the vacuum chamber through side valves.

The statistical uncertainties in the measured values of the absolute elastic differential cross sections result from the statistical variations in the relative flow rates of xenon and helium, the scattered electron yields and the incident electron current. The uncertainty in the theoretical elastic cross section for helium is taken to be 1%. For a given electron energy and scattering angle a series of several measurements were taken and the statistical uncertainty in the differential cross sections was estimated to be 15%.

III. RESULTS AND DISCUSSION

A. Differential cross sections

The differential cross sections measured in the present work at the energies of 5, 7.9, and 10 eV are shown in Figs.

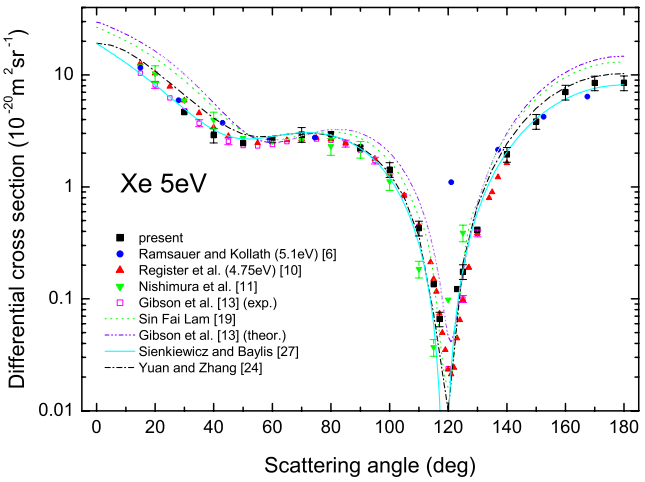

FIG. 1. (Color online) Differential cross sections for electron elastic scattering in xenon at the energy of 5 eV: ■—present results. In the figure are shown experimental results of Ramsauer and Kollath [6], Register *et al.* [10], Nishimura *et al.* [11], and Gibson *et al.* [13] and theoretical results of Sin Fai Lam [19], Gibson *et al.* [13], Sienkiewicz and Baylis [27], and Yuan and Zhang [24].

1–3, respectively. These results cover a wide scattering angle range from 30° to 180°. Also shown are previous experimental cross sections [6,10,11,13,14], which extend up to 140° except those of Ramsauer and Kollath [6], which reach 167.5°. The presented experimental cross sections are compared with the available results from several theoretical calculations [13,14,17,19,24,27]. Where the theoretical results have been reported in terms of elastic scattering phase shifts we have calculated the corresponding cross sections from the partial waves formulas. The present experimental differential cross sections are also presented in Table I.

At the energy of 5 eV (Fig. 1) the present cross sections are in excellent accord with the more recent measurements of

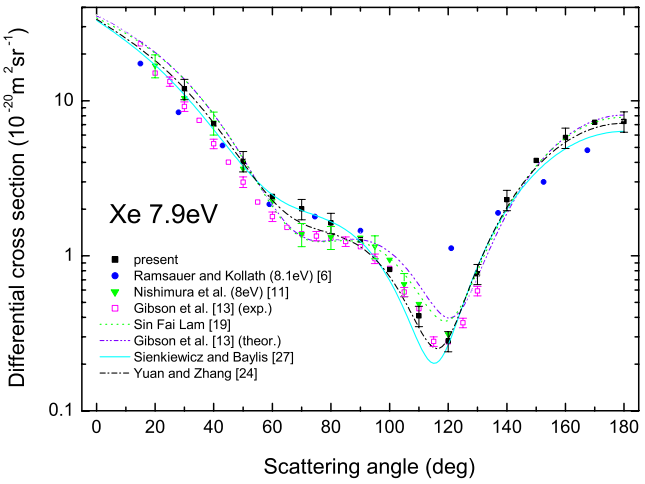

FIG. 2. (Color online) Differential cross sections for electron elastic scattering in xenon at the energy of 7.9 eV: ■—present results. In the figure are shown experimental results of Ramsauer and Kollath [6], Nishimura *et al.* [11], and Gibson *et al.* [13] and theoretical results of Sin Fai Lam [19], Gibson *et al.* [13], Sienkiewicz and Baylis [27], and Yuan and Zhang [24].

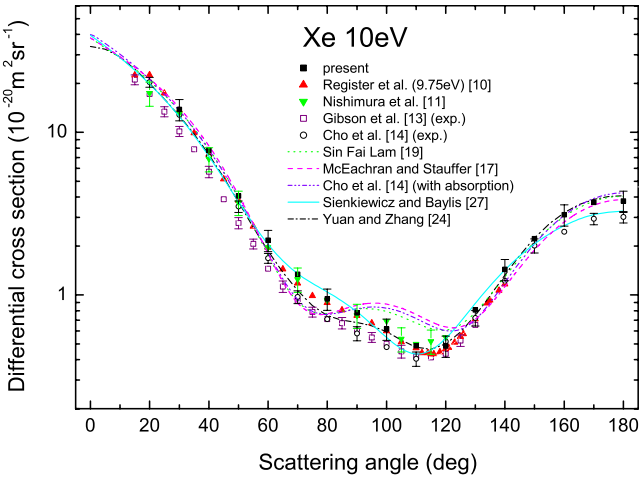

FIG. 3. (Color online) Differential cross sections for electron elastic scattering in xenon at the energy of 10 eV: ■—present results. In the figure are shown experimental results of Register *et al.* [10], Nishimura *et al.* [11], Gibson *et al.* [13], and Cho *et al.* [14], and theoretical results of Sin Fai Lam [19], McEachran and Stauffer [17], Cho *et al.* [14] (with absorption), Sienkiewicz and Baylis [27], and Yuan and Zhang [24].

Register *et al.* [10] (measured at 4.75 eV) and the very recent results of Gibson *et al.* [13] in the angular region where the measurements overlap. In the region above 150° our results agree surprisingly well with the very early cross sections of

TABLE I. Differential cross sections, in units of 10^{-20} m^2 sr^{-1}, for elastic electron scattering in xenon at incident electron energies of 5, 7.9, and 10 eV.

	Electron energy		
Scattering angle (deg)	5 eV	7.9 eV	10 eV
30	4.642	11.94	13.830
40	2.898	7.103	7.760
50	2.460	4.085	4.062
60	2.650	2.412	2.173
70	2.940	2.008	1.339
80	2.965	1.631	0.945
90	2.249	1.263	0.777
100	1.428	0.817	0.618
110	0.429	0.410	0.487
115	0.135		
117	0.066		
120		0.282	0.486
123	0.123		
125	0.175		
130	0.415	0.765	0.809
140	1.953	2.299	1.438
150	3.841	4.115	2.221
160	7.028	5.788	3.117
170	8.481	7.266	3.712
180	8.509	7.363	3.778

Ramsauer and Kollath [6] (measured for electron energy of 5.1 V). The results of Nishimura *et al.* [11] agree well with the above measurements up to 100°, where they start to diverge showing a sharp dip in the differential cross section at a slightly lower angle. The relative measurements of Heindorff *et al.* [8] (not shown in Fig. 1) agree well in their shape with the absolute measurements of Refs. [10,13]. However, their cross section at the minimum of the dip at 120° suffers from low angular resolution of the measurements. Comparison with theoretical investigations reveals that the calculations of Sienkiewicz and Baylis [27] and Yuan and Zhang [24] follow closely and give the best agreement with the experimental cross sections over the whole angular range 15°–180° covered by the measurements. Both the quasirelativistic [24] and relativistic [27] calculations used model potentials to account for correlation-polarization interactions and treated exchange exactly. The largest deviations from the experimental cross sections occur with the polarized-orbital calculations of Sin Fai Lam [19] and those of Gibson *et al.* [13]. The latter calculations differ very little from the previous relativistic (with nonrelativistic polarization potential) results of McEachran and Stauffer [17], which also deviate from the experimental results. These calculations overestimate the experimental cross sections by about 60% at 180° and by a factor of 2 for forward scattering. They also differ significantly from, for example, the results of Sienkiewicz and Baylis, especially in the regions of low and high scattering angles.

At the energy of 7.9 eV (Fig. 2), which is the energy of the $^2P_{3/2}$ resonance in xenon, the present differential cross sections below 60° are in agreement with the previous measurements of Nishimura *et al.* [11] but lie on the average 10–20% above those of Gibson *et al.* [13]. Around 70° our cross section is significantly larger than both the other measurements. However, above 90°, and in the region of overlap up to 130°, all three sets of measurements are in good agreement. At scattering angles above 150° our results are consistently higher than those of Ramsauer and Kollath [6] (measured for an electron energy of 8.1 V). The results of the four theoretical approaches [13,19,24,27] shown in Fig. 2 agree rather well with each other and also with the measured cross sections except in the angular range between 55° and 125° where they diverge from the experimental cross sections. Here, the results of Sienkiewicz and Baylis [27] and Yuan and Zhang [24] better reproduce the shape of the angular dependence of the measured cross sections, including the present ones. Of note is the good agreement at 7.9 eV between all presented results of the calculations, including those of the polarized-orbital approach [13,19], and the present cross section in the backscattering region.

Our 10 eV cross sections (Fig. 3) are in excellent agreement with the measurements of Register *et al.* [10] (measured at 9.75 eV) and Nishimura *et al.* [11] over the angular range 30°–140°. The recent measurements of Gibson *et al.* [13] are lower than the above three experimental studies by about 20% in the range up to 100° where they then start to converge with the other measurements. Comparison of the present measurements with the cross sections measurements of Cho *et al.* [14] in the scattering angle range 20°–180° shows good agreement up to 50° and between 110° and 140°. However, at the intermediate angles our results are higher by about 40%. In the region of backscattering beyond 150° our cross section exceeds that of Cho *et al.* by about 25%. Turning to a comparison with the theoretical cross sections, Fig. 3 clearly indicates that the best agreement with our cross sections is given by the calculations of Sienkiewicz and Baylis [27], disregarding differences close to 180°. The results of Yuan and Zhang [24] also coincide well with our cross sections and those of Register *et al.* [10] and Nishimura *et al.* [11]. Both calculations used model potentials for polarization-correlation interactions. The polarized-orbital approaches of Refs. [14,17,19] deviate from the experimental cross sections in the intermediate scattering angle range 90°–120° but reproduce well the experimental cross sections in the regions of low and high scattering angles.

TABLE II. Integral cross section σ_t and momentum transfer cross section σ_m, in units of 10^{-20} m^2, for elastic electron scattering in xenon.

Energy (eV)	σ_t	σ_m
5	34.3	28.2
7.9	44.4	26.4
10	42.3	18.8

B. Integral and momentum transfer cross sections

We have deduced the integral cross section σ_t and the momentum transfer cross section σ_m for elastic scattering at electron energies of 5, 7.9, and 10 eV. For these, the differential cross sections have been integrated over the scattering angle range 0°–180° after extrapolating the present cross sections from 30° down to 0°. In this extrapolation procedure we have assumed the angular dependencies of the differential cross sections calculated by Sienkiewicz and Baylis [27]. The resultant integral cross sections are listed in Table II. The associated uncertainties of the integral elastic and momentum transfer cross sections are equal to 17% and 15%, respectively, and are deduced from the uncertainties of our measured differential cross sections. The extrapolation procedure for the low-angle cross sections introduces an uncertainty of less than 2% into the integral cross section and less than 0.1% into the momentum transfer cross section. The present integral cross section is compared in Fig. 4 with the available values from measured total cross sections [34–41], determinations from the differential cross sections measurements [11,13], and theoretical cross sections [18–20,27]. Our momentum transfer cross section is shown in Fig. 5 together with cross sections determined from swarm measurements [42–45], experimental [10,11,13,14], and calculated [14,18,19,27] differential cross sections and the preferred cross sections as given in the subvolume "Interactions of Photons and Electrons with Atoms" of Landolt-Börnstein [46].

The present integral cross sections at the energies of 5, 7.9, and 10 eV (Fig. 4) are in very good agreement with the previously measured total cross sections [35,36,38,39,41].

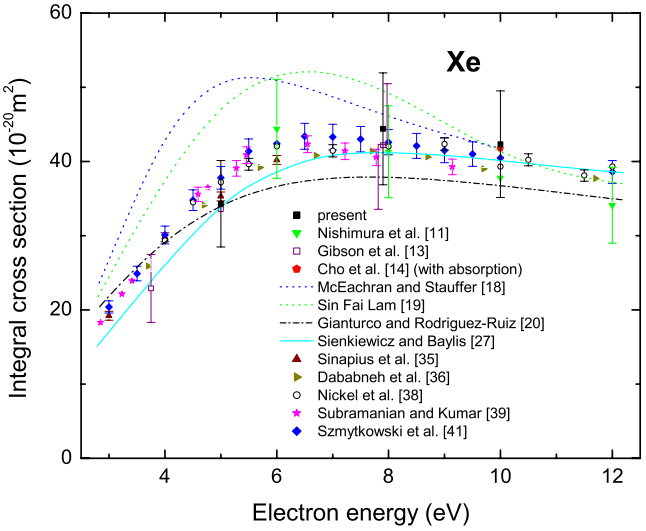

FIG. 4. (Color online) Integral cross sections for elastic electron scattering in xenon: ■—present results. In the figure are shown experimental results of Nishimura *et al.* [11] and Gibson *et al.* [13], theoretical results of Cho *et al.* [14] (with absorption), McEachran and Stauffer [18], Sin Fai Lam [19], Gianturco and Rodriguez-Ruiz [20], and Sienkiewicz and Baylis [27], and experimental total cross sections of Sinapius *et al.* [35], Dababneh *et al.* [36], Nickel *et al.* [38], Subramanian and Kumar [39], and Szmytkowski *et al.* [41].

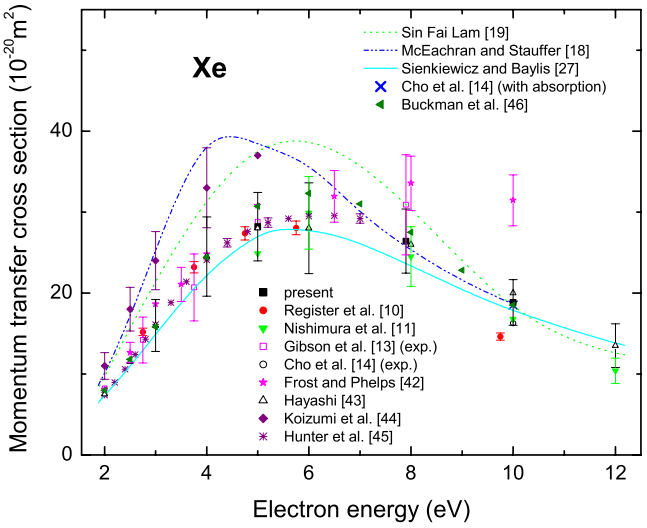

FIG. 5. (Color online) Momentum transfer cross sections in xenon: ■—present results. In the figure are shown experimental results of Register *et al.* [10], Nishimura *et al.* [11], Gibson *et al.* [13], Cho *et al.* [14], Frost and Phelps [42], Hayashi [43], Koizumi *et al.* [44], and Hunter *et al.* [45], theoretical results of McEachran and Stauffer [18], Sin Fai Lam [19], Sienkiewicz and Baylis [27], Cho *et al.* [14] (with absorption), and preferred values of Buckman *et al.* [46].

This is despite the fact that the uncertainties in the integral cross sections deduced from the differential cross sections are generally significantly higher than those of the total cross sections. The total cross section at 10 eV may contain some contribution from the inelastic cross section as it is measured 1.6 eV above the first, ^3P excitation threshold of xenon (at 8.315 eV). However, this contribution is small, $<0.5\%$ [43] and allows for comparison of the total cross sections with our integral elastic cross section. From the integration of the differential cross sections it is found that the contributions from scattering above 120° to the integral cross section are significant and equal to 24%, 19%, and 12% for energies of 5, 7.9, and 10 eV, respectively. From comparison with the theoretical integral elastic cross sections it is clear again that the results of Sienkiewicz and Baylis [27] are in the best agreement with the measurements. The polarized-orbital calculations [18,19] tend to overestimate the cross section in the energy range 3–8 eV.

The momentum transfer cross section (Fig. 5) obtained in the present work at 5 eV agrees very well with the cross sections determined from the swarm experiment of Hunter *et al.* [45] and with the recommended cross section derived from swarm and cross-beam experiments by Hayashi [43]. At 7.9 and 10 eV we agree well with the cross section of Hayashi and also those of Nishimura *et al.* [11] and Cho *et al.* [14] (at 10 eV), which were deduced from their angular measurements. We observe in the integration of the differential cross sections that the angular range 120°–180° introduces a 50–60% contribution to the momentum transfer cross section. From the deduced momentum transfer cross sections we can conclude that the best agreement with experiment over the whole energy range is provided by the calculations of Sienkiewicz and Baylis [27]. This was similarly the case for the integral elastic cross section.

IV. CONCLUSIONS

We have measured differential cross sections for elastic electron scattering from xenon over a wide scattering angle range 30°–180°, at the energies of 5, 7.9, and 10 eV. For the energies lying below the first excitation threshold (8.315 eV) these are the first results obtained in the region of 180°. Comparison with the theoretical results reveals that approaches applying model polarization potentials (Yuan and Zhang [24], Sienkiewicz and Baylis [27]) are in good accord with the experimental cross sections in the whole scattering angle range. In the scattering region above 130° the polarized-orbital calculations overestimate the cross sections at 5 eV but unlike the case of argon, are in agreement with our experimental results at 7.9 and 10 eV.

The integral elastic and momentum transfer cross sections have been derived from the present results at 5, 7.9, and 10 eV through integration over the total angular range 0°–180°. The present integral cross section is in good agreement with the absolute total cross section measurements despite the fact that its estimated uncertainty (17%) is nearly five times greater than the uncertainties associated with the total cross section measurements. The preferred values of the momentum transfer cross section given in the subvolume "Interactions of Photons and Electrons with Atoms" of Landolt-Börnstein [46] are in reasonable agreement with the determinations of this cross section in the present work and Refs. [43,45].

ACKNOWLEDGMENTS

The authors are grateful to R. P. McEachran for providing tabulated results of the calculated cross sections published in [13,14]. This work has been partly supported by the Polish State Committee for Scientific Research and by the Engineering and Physical Sciences Research Council of the UK. One of us (I.L.) is grateful to British Council for a grant under the Young Scientists Programme.

[1] M. Zubek, A. Danjo, and G. C. King, J. Phys. B **28**, 4117 (1995).
[2] A. Zecca, G. P. Karwasz, and R. S. Brusa, Riv. Nuovo Cimento **19**, 1 (1996).
[3] B. Mielewska, I. Linert, G. C. King, and M. Zubek, Phys. Rev. A **69**, 062716 (2004).
[4] I. Linert, B. Mielewska, G. C. King, and M. Zubek, Phys. Rev. A **74**, 042701 (2006).
[5] I. Linert, G. C. King, and M. Zubek, J. Electron Spectrosc. Relat. Phenom. **134**, 1 (2003).
[6] C. Ramsauer and R. Kollath, Ann. Phys. **12**, 837 (1932).
[7] J. Mehr, Z. Phys. **198**, 345 (1967).
[8] T. Heindorff, J. Höfft, and P. Dabkiewicz, J. Phys. B **9**, 89 (1976).
[9] M. Klewer, M. J. M. Beerlage, and M. J. van der Wiel, J. Phys. B **13**, 571 (1980).
[10] D. F. Register, L. Vuskovic, and S. Trajmar, J. Phys. B **19**, 1685 (1986).
[11] H. Nishimura, T. Matsuda, and A. Danjo, J. Phys. Soc. Jpn. **56**, 70 (1987).
[12] M. Weyhreter, B. Barzick, A. Mann, and F. Linder, Z. Phys. D: At., Mol. Clusters **7**, 333 (1988).
[13] J. C. Gibson, D. R. Lun, L. J. Allen, R. P. McEachran, L. A. Parcell, and S. J. Buckman, J. Phys. B **31**, 3949 (1998).
[14] H. Cho, R. P. McEachran, S. J. Buckman, D. M. Filipović, V. Pejcev, B. P. Marinković, H. Tanaka, A. D. Stauffer, and E. C. Jung, J. Phys. B **39**, 3781 (2006).
[15] W. D. Walker, Adv. Phys. **20**, 257 (1971).
[16] R. P. McEachran and A. D. Stauffer, J. Phys. B **17**, 2507 (1984).
[17] R. P. McEachran and A. D. Stauffer, J. Phys. B **19**, 3523 (1986).
[18] R. P. McEachran and A. D. Stauffer, J. Phys. B **20**, 3483 (1987).
[19] L. T. Sin Fai Lam, J. Phys. B **15**, 119 (1982).
[20] F. A. Gianturco and J. A. Rodriguez-Ruiz, Z. Phys. D: At., Mol. Clusters **31**, 149 (1994).
[21] R. Haberland, L. Fritsche, and J. Noffke, Phys. Rev. A **33**, 2305 (1986).
[22] W. R. Johnson and C. Guet, Phys. Rev. A **49**, 1041 (1994).
[23] J. Yuan and Z. Zhang, J. Phys. B **22**, 2581 (1989).
[24] J. Yuan and Z. Zhang, J. Phys. B **24**, 275 (1991).
[25] N. T. Padial and D. W. Norcross, Phys. Rev. A **29**, 1742 (1984).
[26] J. K. O'Connell and N. F. Lane, Phys. Rev. A **27**, 1893 (1983).
[27] J. E. Sienkiewicz and W. E. Baylis, J. Phys. B **22**, 3733 (1989).
[28] H. P. Berg, Phys. Lett. **88A**, 292 (1982).
[29] F. H. Read and J. M. Channing, Rev. Sci. Instrum. **67**, 2372 (1996).
[30] I. Linert, G. C. King, and M. Zubek, J. Phys. B **37**, 4681 (2004).
[31] R. K. Nesbet, Phys. Rev. A **20**, 58 (1979).
[32] M. A. Khakoo and S. Trajmar, Phys. Rev. A **34**, 138 (1986).
[33] J. C. Nickel, C. Mott, I. Kanik, and D. C. McCollum, J. Phys. B **21**, 1867 (1988).
[34] C. Ramsauer, Ann. Phys. **72**, 345 (1923).
[35] G. Sinapius, W. Raith, and W. G. Wilson, J. Phys. B **13**, 4079 (1980).
[36] M. S. Dababneh, W. E. Kauppila, J. P. Downing, F. Laperriere, V. Pol, J. H. Smart, and T. S. Stein, Phys. Rev. A **22**, 1872 (1980).
[37] K. Jost, P. G. F. Bisling, F. Eschen, M. Felsmann, and L. Walther, in *Proceedings of the 13th International Conference on the Physics of Electronic and Atomic Collisions*, edited by J. Eichler (North-Holland, Amsterdam, 1983), p. 91.
[38] J. C. Nickel, K. Imre, D. F. Register, and S. Trajmar, J. Phys. B **18**, 125 (1985).
[39] K. P. Subramanian and V. Kumar, J. Phys. B **20**, 5505 (1987).
[40] D. T. Alle, M. J. Brennan, and S. J. Buckman, in *Proceedings of the 18th International Conference on the Physics of Electronic and Atomic Collisions*, edited by T. Andersen, B. Fastrup, F. Folkmann, and H. Knudsen (Aarhus University, 1993), p. 127.
[41] C. Szmytkowski, K. Maciag, and G. Karwasz, Phys. Scr. **54**, 271 (1996).
[42] L. S. Frost and A. V. Phelps, Phys. Rev. **136**, A1538 (1964).
[43] M. Hayashi, J. Phys. D **16**, 581 (1983).
[44] T. Koizumi, E. Shirakawa, and I. Ogawa, J. Phys. B **19**, 2331 (1986).
[45] S. R. Hunter, J. G. Carter, and L. G. Christophorou, Phys. Rev. A **38**, 5539 (1988).
[46] S. J. Buckman, J. W. Cooper, M. T. Elford, M. Inokuti, Y. Itikawa, and H. Tawara, edited by Y. Itikawa, in *Landolt-Börnstein, Numerical Data and Functional Relationships in Science and Technology*, New Series Group I/17A (Springer, Berlin, 2000).